Multiple perceptible signals from a single olfactory glomerulus

Matthew Smear[1], Admir Resulaj[1,2], Jingji Zhang[3], Thomas Bozza[3] & Dmitry Rinberg[1,2]

Glomeruli are functional units in the olfactory system. The mouse olfactory bulb contains roughly 2,000 glomeruli, each receiving inputs from olfactory sensory neurons (OSNs) that express a specific odorant receptor gene. Odors typically activate many glomeruli in complex combinatorial patterns and it is unknown which features of neuronal activity in individual glomeruli contribute to odor perception. To address this, we used optogenetics to selectively activate single, genetically identified glomeruli in behaving mice. We found that mice could perceive the stimulation of a single glomerulus. Single-glomerulus stimulation was also detected on an intense odor background. In addition, different input intensities and the timing of input relative to sniffing were discriminated through one glomerulus. Our data suggest that each glomerulus can transmit odor information using identity, intensity and temporal coding cues. These multiple modes of information transmission may enable the olfactory system to efficiently identify and localize odor sources.

The glomeruli of the olfactory bulb are the input channels of the olfactory system, where OSNs connect to the brain[1–3]. A given glomerulus receives input from OSNs expressing a given odorant receptor gene[4–6], of which there are approximately 1,000 encoded in the mouse genome. The large size of the odorant receptor gene family endows the glomerular array with an identity code of enormous combinatorial capacity[7,8]. In addition to this combinatorial identity code, individual glomeruli convey information about odor stimuli in their amplitude of activation[9–11] and the timing of activity relative to the sniff cycle[12–14]. However, given that odors typically evoke activity from many glomeruli[7,9,11,15,16], it has not been possible to determine the contribution of single glomeruli to odor perception.

To determine how a single glomerulus contributes to perception, we used optogenetics to express channelrhodopsin-2 in sensory neurons that express a specific odorant receptor and that project to defined glomeruli. We found that stimulation of a single glomerulus can drive perception, even when many glomeruli are activated simultaneously by an odor stimulus. In addition, we found that different amplitudes of glomerular stimulation can be discriminated, as well as different timing of activation during the sniff cycle. Thus, individual glomeruli can drive behavior using identity, amplitude and temporal coding signals.

RESULTS

To stimulate a single glomerulus, we used gene targeting in the mouse to express a fusion protein of channelrhodopsin-2 and yellow fluorescent protein (ChR2-YFP) in OSNs that expressed the odorant receptor *M72* (also known as *Olfr160*; **Fig. 1a**). OSNs expressing the M72 receptor have been extensively characterized in terms of development, anatomy and function, and their properties are similar to those of other characterized OSN types[17,18]. In these *M72-ChR2*

mice, OSNs that express the native, intact M72 receptor also express ChR2-YFP, making them light sensitive (**Fig. 1a**). The axons of ChR2-YFP–expressing sensory neurons recapitulate the normal pattern of M72 OSN axonal projections, innervating a medial and a lateral glomerulus on the dorsal surface of each olfactory bulb[12].

Next, we measured behavior in response to odorants or light. To deliver light to M72 glomeruli *in vivo*, we chronically implanted *M72-ChR2* mice with an optical fiber positioned over the lateral M72-ChR2 glomerulus in the right hemisphere (**Fig. 1a**). To control for the possibility that light stimuli could be detectable by means other than ChR2 (for example, vision or thermosensation), we implanted a second optical fiber just caudal to the olfactory bulb in the left hemisphere (**Fig. 1a**). To measure sniffing, we implanted a pressure cannula into the left nasal cavity (**Fig. 1b**)[14].
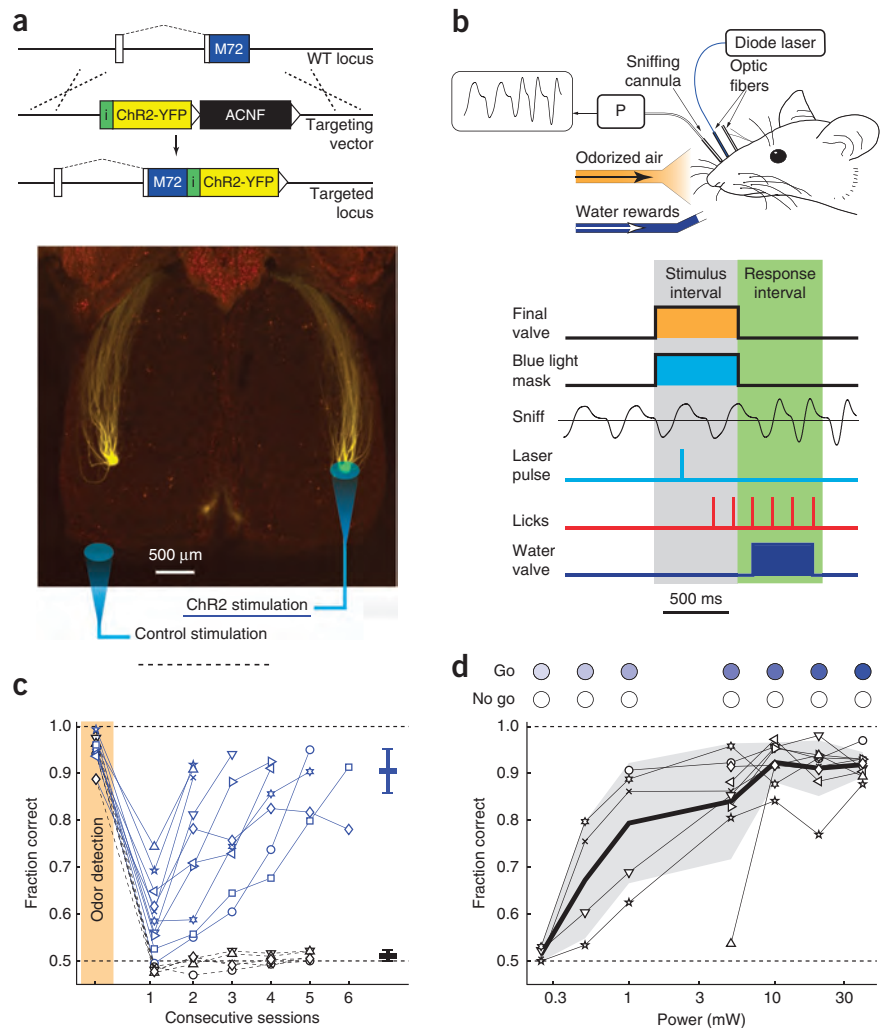
We trained *M72-ChR2* mice to report perceptual judgments in a head-fixed, go/no-go task[19] (**Fig. 1b** and **Supplementary Table 1**). After initially training mice to report the detection of odors (**Fig. 1c**), we asked whether mice could detect light-driven olfactory input through a single glomerulus. When light was used to drive activation of a single M72-ChR2 glomerulus (40-mW power, 10-ms duration), 10 of 11 mice learned to report detection (two-sided binomial test, $P < 0.01$; **Fig. 1c**). All of the mice that detected this stimulus learned quickly, achieving high performance after 2–5 sessions. In contrast, when stimulated via the control fiber, all of the mice ($n = 5$) failed to report light detection above chance level in five consecutive sessions (two-sided binomial test, $P > 0.29$; **Fig. 1c**). Thus, mice can perceive activation of OSN inputs to a single olfactory glomerulus, which we refer to as monoglomerular stimulation.

To determine the sensitivity of mice to monoglomerular stimulation, we measured detection performance with varying light intensity

Figure 1 Stimulating single olfactory glomeruli with light. (**a**) Top, diagram of the gene targeting strategy. An internal ribosome entry site (IRES, green box) was inserted into the gene encoding the olfactory receptor M72 just after the unmodified receptor coding sequence. The IRES was followed by the coding sequence for ChR2-YFP (yellow box). In *M72-ChR2* mice, ChR2-YFP labels M72-expressing OSNs and their axons in the bulb. Bottom, convergence of M72 axons into single glomeruli in the left and right olfactory bulbs is shown in a dorsal view whole mount. YFP-labeled medial glomeruli can also be seen. The diagram indicates the optical fiber placement above the right lateral M72 glomerulus for ChR2 stimulation and above the frontal cortex for control stimulation. (**b**) Top, schematic of experimental setup. Mice were implanted with two optic fibers to deliver light and a sniffing cannula coupled to a pressure sensor (P) to measure sniffing. Inverted intranasal pressure signal is shown at top left. Bottom, behavioral trial structure. (**c**) Performance of *M72-ChR2* mice in an odor detection session, followed by light detection sessions with ChR2 stimulation (blue symbols, $n = 10$ mice) and control stimulation sessions (black circles, $n = 5$ mice). Symbols at far right represent across-mouse mean ± s.d. (**d**) Detection as a function of stimulus power. Black symbols indicate the performance of individual *M72-ChR2* mice, whereas the black line and shaded region represent the mean ± s.d. for all mice ($n = 9$). Horizontal dashed lines represent the range of performance change from chance level to maximum.

and a fixed stimulus duration (1 ms). For the majority of mice (8 of 9), detection performance was high over a range of light stimulus powers (5–40 mW; **Fig. 1d**). Performance decreased at 1 mW, reaching chance level at 250 µW (two-sided binomial test, $P > 0.18$; **Fig. 1d**).

Odors typically activate multiple glomeruli[7,9,11,15,16]. Can stimulation of a single glomerulus be detected in the presence of other odor-activated glomeruli? To approach this question, we measured the detection of monoglomerular stimulation in the presence of odors that do or do not activate the odorant receptor M72. We reasoned that M72 ligands should mask light detection, whereas odorants that do not activate M72 should not affect light detection. Using perforated-patch recordings from M72-expressing OSNs, we identified a set of ligands (methyl salicylate, ethyl tiglate and methyl benzoate) that evoked large odorant transduction currents and another set of non-ligands (+-carvone, hexanal and octanoic acid) that did not evoke a response (**Fig. 2a,b**). We then performed behavioral experiments in which we presented these odorants at a high concentration (10^{-3} dilution of saturated vapor pressure) so that they would activate many glomeruli[10,16]. Using these stimuli, we tested a set of mice in sessions in which they received a 500-ms odor pulse paired with light (go stimulus) and an odor pulse without light (no-go stimulus). We used a light stimulus power for which detection performance was >75% in the absence of odor (1 or 20 mW for individual mice, depending on their performance). Only one odor was used in each session. Sessions with odor and light alternated with sessions with only light and no paired odor (Online Methods).

We tested light detection when M72 ligands were used as the paired odor stimulus (**Fig. 2c**). As predicted, light detection performance in the presence of M72 ligands was significantly decreased compared with the odorless condition ($n = 5$ mice, $P < 0.0061$, two-tailed t test; **Fig. 2d**). This masking result indicates that light-evoked activity is within the same range of intensity as odor-evoked activity. Notably, in the presence of one M72 ligand, methyl benzoate, detection performance did not drop to chance, and increasing light power further increased performance (**Supplementary Fig. 1**). This residual detection performance indicates that, at this concentration, methyl benzoate does not saturate the signaling capacity of M72 glomeruli.

We next tested light detection in the presence of M72 non-ligands. Under this condition, we observed that mice could easily detect stimulation of M72 glomeruli (**Fig. 2c**). This detection performance was statistically indistinguishable from detection of M72 stimulation in the absence of odor ($P > 0.25$, paired t test; **Fig. 2d**). Notably, these experiments, in which M72 non-ligands did not mask light detection, used the same light intensity and odor dilution as experiments in which M72 ligands did mask light detection. Taken together, this odor-specific masking indicates that M72 ligands and light are perceived via the same input channel, further reinforcing the idea that light stimuli are sensed by the olfactory system and not by another modality. Furthermore, our finding that monoglomerular stimulation can be detected against an odor background indicates that mice can perceive the smallest possible change to a spatial pattern of odor-evoked glomerular input.
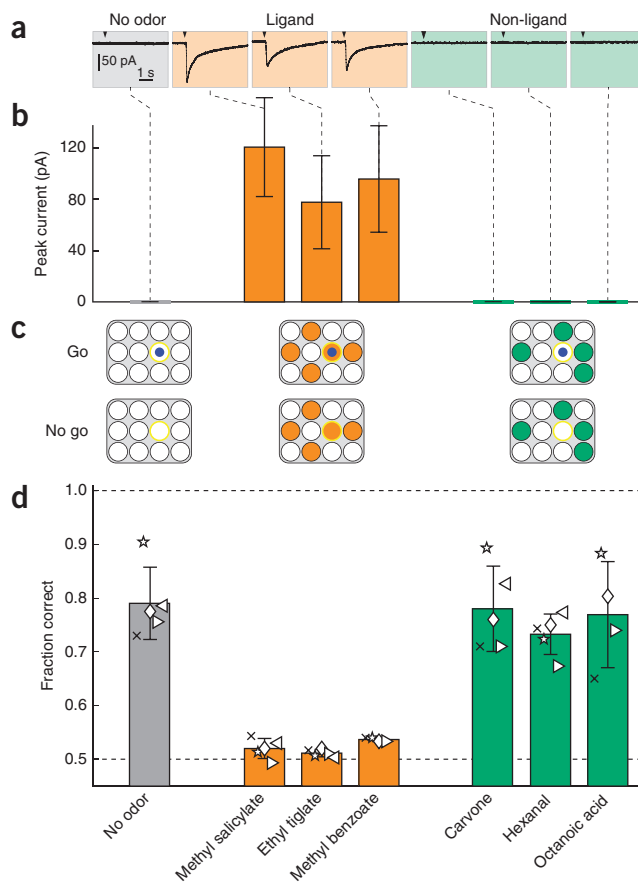
In addition to spatial patterns of activated glomeruli, the graded response amplitudes of individual glomeruli carry information about

Figure 2 Detecting monoglomerular activation paired with odor.
(**a**) Example traces showing odor-induced currents from M72-expressing
OSNs. (**b**) Average odor-evoked current amplitudes (mean ± s.d.,
$n = 10$ cells). (**c**) Schematic of responses of the glomerular array (circles)
to paired odor and light stimuli. The yellow circle denotes the M72-ChR2
glomerulus and the blue dot indicates light stimulation. M72 ligands
activated the M72-ChR2 glomerulus and other glomeruli (orange-filled
circles). Non-M72 ligands activated other glomeruli (green-filled circles),
but not the M72-ChR2 glomerulus. (**d**) Light detection performance in
the presence of different odors. Black symbols indicate performance
for individual mice. Error bars represent across-mouse mean ± s.d. for
performance in the presence of no odor (gray), M72 ligands (orange)
and M72 non-ligands (green). Horizontal dashed lines represent the range
of performance change from chance level to maximum.

odor identity and intensity[9–11]. However, it is not known whether
graded activation of a single glomerulus is perceptually accessible. We
therefore asked whether mice could discriminate monoglomerular
stimulation of different intensities, an experiment that is not possible
using odors because increasing odor concentration recruits larger
numbers of glomeruli[9,15]. In the detection experiments described
above (**Fig. 1d**), we defined a range of laser powers (1–20 mW)
that evoked suprathreshold detection behavior. Can mice discrim-
inate between light powers drawn from this suprathreshold range
(**Fig. 3a**)? We tested whether mice ($n = 6$) could discriminate a high
power (20 mW) from lower powers (1, 5 and 10 mW), all of which
evoked >75% detection performance (**Fig. 1d**). In each trial, a single
light pulse was delivered, and only the light power was varied across
trials. We observed that mice could readily discriminate input inten-
sity using a single glomerulus. Performance decreased with the ratio
of light intensity (**Fig. 3a**), with above-chance performance being
maintained for discriminations between powers that were detected
at a high performance level (two-sided binomial test, $P < 0.01$ for 3 of
6 mice for discrimination between 20- and 10-mW laser power).
Taken together, our results suggest that mice can sense intensity
differences from a single glomerulus, indicating that the signaling
capacity of the glomerulus is graded, rather than all or nothing.

Olfactory neurons also encode information in the timing of their
responses relative to the sniff cycle[12–14]. We previously found that
mice can sense the timing of olfactory input with respect to sniffing
(sniff phase) for stimuli that activate many glomeruli[19]. Can mice
perceive sniff phase cues using a single glomerulus (**Fig. 3b**)? To test
this, we asked whether mice ($n = 4$) could discriminate between iden-
tical light pulses (20-mW power, 1-ms duration) that differed only
in the time of presentation relative to the sniff cycle. Go stimuli were
delivered 25 ms after the onset of inhalation and no-go stimuli were
triggered after a longer latency (see Online Methods and **Fig. 3b**). The
mice discriminated monoglomerular sniff phase cues with high tem-
poral precision, demonstrating above-chance performance at latency
differences as small as 25 ms (two-sided binomial test, $P < 0.002$,
Fig. 3b). This behavioral performance indicates that sniff phase
signaling can be perceptually decoded from a single glomerulus.

Are sniff phase and amplitude distinct signals? Given that OSN
activity is modulated by nasal airflow[20,21], it is possible that sniff
phase differences may be transformed into amplitude differences at
the level of OSNs. To test whether sniff phase and amplitude signals
are distinct, we measured sniff phase discrimination (50-ms latency
difference) across a range of randomly interleaved stimulus powers
(5, 10 and 20 mW), among which mice were able to discriminate
(**Fig. 3a**). If mice sensed the amplitude of input rather than timing,
the performance of the latency discrimination task would depend
on amplitude. Contrary to this prediction, latency discrimination
performance varied only slightly with stimulus intensity (**Fig. 3c**).

Over a fourfold range of stimulus power, discrimination performance
changed by only a few percent (0–5% across three mice), a small frac-
tion of the variation in performance as a function of latency difference
(**Fig. 3b**). This result supports the idea that mice treat sniff phase and
amplitude information as independent signals.

DISCUSSION

The large size of the olfactory receptor repertoire endows olfaction
with an identity code of large combinatorial capacity[7,8]. However, the
degree to which individual glomeruli contribute to odor perception
is unclear. By expressing ChR2 in a single type of OSN, we were able
to study the signaling capacity of a single olfactory glomerulus. We
found that stimulation of OSN inputs to a single glomerulus can be
perceived. Furthermore, this activation can be perceived even when,
at the same time, many glomeruli are driven by a background odor
stimulus. Thus, the smallest change in the glomerular identity code
can be detected, suggesting that the full combinatorial capacity of
the glomerular array is available to perception. For future studies, it
will be interesting to test whether other glomeruli can similarly drive
behavior. In addition, we found that single glomerulus stimulation can
be discriminated solely on the basis of amplitude or timing cues, indi-
cating that the same pattern of glomerular input can be discriminated
on the basis of non-spatial cues. Our data show that an individual
glomerulus, the functional unit of olfactory processing, can contribute
to odor perception by simultaneously relaying identity, intensity and
timing signals, and all of these modes of neuronal coding should be
taken into account when analyzing stimulus representation in the
olfactory system.

As we found in mice, single olfactory inputs can drive behav-
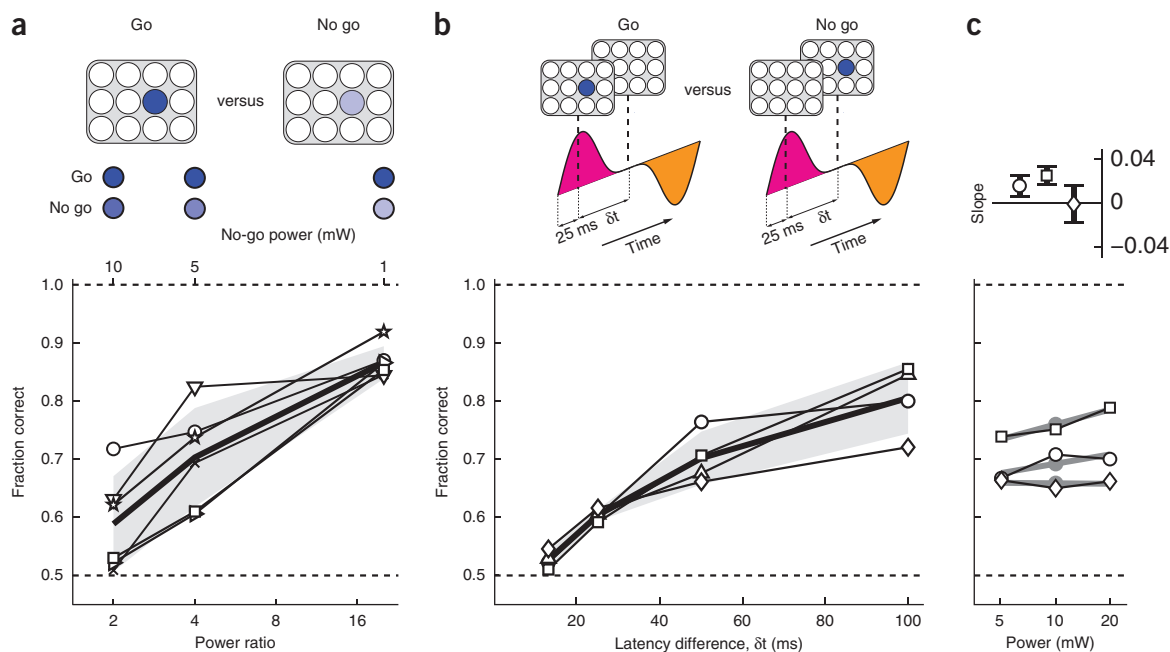ior in *Drosophila*, in which individual glomerular circuits mediate

Figure 3 Discrimination of monoglomerular amplitude and timing differences. (**a**) Monoglomerular amplitude discrimination. Mice discriminated a high stimulus power (dark blue, go stimulus) from lower stimulus powers (light blue, no-go stimulus). Black symbols indicate the performance of individual mice as a function of the ratio between high and low powers. The thick black line and shaded region represent the mean ± s.d. (*n* = 5 mice). (**b**) Discrimination as a function of latency difference. The diagram shows light input as a function of time in sniff cycle. Inhalation (pink) and exhalation (orange) are indicated. Mice discriminated laser pulses delivered at a short latency relative to inhalation onset (go) from pulses that occurred at longer latencies (no go). Black symbols indicate the performance of individual mice as a function of latency difference. The thick black line and shaded region represent the mean ± s.d. (*n* = 4). (**c**) Sniff timing discrimination at multiple stimulus powers. Black symbols indicate the performance of individual mice discriminating a single latency difference (50 ms) as a function of stimulus power. The gray lines represent best-fit lines obtained by logistic regression. Top, slopes in $\log_2$(power) coordinates ±95% confidence interval for individual mice. Horizontal dashed lines represent the range of performance change from chance level to maximum.

hardwired attraction or aversion behaviors[22–24]. In addition, flies can learn to discriminate odors using only a single class of olfactory sensory neuron[37]. Our results indicate that single olfactory input channels are relevant to learned behavior in a mammalian olfactory system with two orders of magnitude more glomeruli. Our findings on the signaling capacity of single glomeruli may help to explain the impressive ability of the mammalian olfactory system to discriminate subtly different odorant mixture stimuli[25–27].

How do olfactory circuits downstream of the OSNs process monoglomerular input? In addition to activating the postsynaptic neurons that arborize in the M72 glomerulus, lateral circuitry in the olfactory bulb may spread monoglomerular stimulation, thereby influencing activity in second-order neurons associated with other glomeruli. This lateral communication may be mediated by inhibitory circuits in the olfactory bulb[28,29] or by lateral excitation[30]. Thus, perception of monoglomerular inputs could involve activation of output cells from additional glomeruli. Further work will be required to characterize olfactory bulb neuronal responses to photic monoglomerular stimuli.

Downstream of the olfactory bulb, recent physiological studies suggest that neurons in piriform cortex integrate across multiple glomeruli and are poorly driven by activity in single glomeruli[31,32]. Our findings indicate that stimulation of a single glomerulus can drive downstream circuits and odor perception. There are several possible explanations for this seeming discrepancy. Although unlikely, it is formally possible that the behavior that we measured may not be mediated by piriform cortex; the olfactory bulb projects to multiple target structures[33], which could underlie the behavior we observe. Another possibility is that piriform responses may be absent in naive animals, but are recruited

by learning-related plasticity; over the course of training sessions, our mice improved at monoglomerular detection. A final possibility is that the aforementioned physiological studies used anesthetized mice. Anesthesia is known to markedly change the spontaneous and odor-evoked activity of the olfactory bulb[34,35]. In light of this, monoglomerular stimulation in awake, behaving mice will be a powerful tool for deciphering odor coding by central olfactory circuits.

Our results are consistent with a scheme in which olfactory perception can use the full combinatorial capacity of the glomerular array and the idea that this capacity is extended by graded signaling in the amplitude and sniff phase domains. Why does the olfactory system have so much signaling capacity? We propose that this richness has evolved to provide the best possible representation of complex natural olfactory scenes, in which multiple odor sources emit numerous volatile molecules, which propagate to the nose by turbulent flow. For example, sophisticated sensing through individual glomeruli may help to overcome olfactory 'cocktail party' problems such as perceiving faint scents in the presence of multiple odor sources[36].

METHODS

Methods and any associated references are available in the online version of the paper.

Note: Any Supplementary Information and Source Data files are available in the online version of the paper.

1. Hildebrand, J.G. & Shepherd, G.M. Mechanisms of olfactory discrimination: converging evidence for common principles across phyla. *Annu. Rev. Neurosci.* **20**, 595–631 (1997).
2. Mori, K. The olfactory bulb: coding and processing of odor molecule information. *Science* **286**, 711–715 (1999).
3. Wilson, R.I. & Mainen, Z.F. Early events in olfactory processing. *Annu. Rev. Neurosci.* **29**, 163–201 (2006).
4. Ressler, K.J., Sullivan, S.L. & Buck, L.B. Information coding in the olfactory system: evidence for a stereotyped and highly organized epitope map in the olfactory bulb. *Cell* **79**, 1245–1255 (1994).
5. Vassar, R. *et al.* Topographic organization of sensory projections to the olfactory bulb. *Cell* **79**, 981–991 (1994).
6. Mombaerts, P. *et al.* Visualizing an olfactory sensory map. *Cell* **87**, 675–686 (1996).
7. Malnic, B., Hirono, J., Sato, T. & Buck, L.B. Combinatorial receptor codes for odors. *Cell* **96**, 713–723 (1999).
8. Koulakov, A., Gelperin, A. & Rinberg, D. Olfactory coding with all-or-nothing glomeruli. *J. Neurophysiol.* **98**, 3134–3142 (2007).
9. Rubin, B.D. & Katz, L.C. Optical imaging of odorant representations in the mammalian olfactory bulb. *Neuron* **23**, 499–511 (1999).
10. Bozza, T., McGann, J.P., Mombaerts, P. & Wachowiak, M. *In vivo* imaging of neuronal activity by targeted expression of a genetically encoded probe in the mouse. *Neuron* **42**, 9–21 (2004).
11. Wachowiak, M. & Cohen, L.B. Representation of odorants by receptor neuron input to the mouse olfactory bulb. *Neuron* **32**, 723–735 (2001).
12. Macrides, F. & Chorover, S.L. Olfactory bulb units: activity correlated with inhalation cycles and odor quality. *Science* **175**, 84–87 (1972).
13. Chaput, M. & Holley, A. Single unit responses of olfactory bulb neurones to odor presentation in awake rabbits. *J. Physiol. (Paris)* **76**, 551–558 (1980).
14. Spors, H., Wachowiak, M., Cohen, L.B. & Friedrich, R.W. Temporal dynamics and latency patterns of receptor neuron input to the olfactory bulb. *J. Neurosci.* **26**, 1247–1259 (2006).
15. Stewart, W.B., Kauer, J.S. & Shepherd, G.M. Functional organization of rat olfactory bulb analyzed by the 2-deoxyglucose method. *J. Comp. Neurol.* **185**, 715–734 (1979).
16. Soucy, E.R., Albeanu, D.F., Fantana, A.L., Murthy, V.N. & Meister, M. Precision and diversity in an odor map on the olfactory bulb. *Nat. Neurosci.* **12**, 210–220 (2009).
17. Potter, S.M. *et al.* Structure and emergence of specific olfactory glomeruli in the mouse. *J. Neurosci.* **21**, 9713–9723 (2001).
18. Zhang, J., Huang, G., Dewan, A., Feinstein, P. & Bozza, T. Uncoupling stimulus specificity and glomerular position in the mouse olfactory system. *Mol. Cell Neurosci.* (2012).
19. Smear, M., Shusterman, R., O'connor, R., Bozza, T. & Rinberg, D. Perception of sniff phase in mouse olfaction. *Nature* **479**, 397–400 (2011).
20. Sobel, E.C. & Tank, D.W. Timing of odor stimulation does not alter patterning of olfactory bulb unit activity in freely breathing rats. *J. Neurophysiol.* **69**, 1331–1337 (1993).
21. Carey, R.M., Verhagen, J.V., Wesson, D.W., Pirez, N. & Wachowiak, M. Temporal structure of receptor neuron input to the olfactory bulb imaged in behaving rats. *J. Neurophysiol.* **101**, 1073–1088 (2008).
22. Suh, G.S.B. *et al.* A single population of olfactory sensory neurons mediates an innate avoidance behavior in *Drosophila. Nature* **431**, 854–859 (2004).
23. Semmelhack, J.L. & Wang, J.W. Select *Drosophila* glomeruli mediate innate olfactory attraction and aversion. *Nature* **459**, 218–223 (2009).
24. Stensmyr, M.C. *et al.* A conserved dedicated olfactory circuit for detecting harmful microbes in *Drosophila. Cell* **151**, 1345–1357 (2012).
25. Uchida, N. & Mainen, Z.F. Speed and accuracy of olfactory discrimination in the rat. *Nat. Neurosci.* **6**, 1224–1229 (2003).
26. Abraham, N.M. *et al.* Maintaining accuracy at the expense of speed: stimulus similarity defines odor discrimination time in mice. *Neuron* **44**, 865–876 (2004).
27. Rinberg, D., Koulakov, A. & Gelperin, A. Speed-accuracy tradeoff in olfaction. *Neuron* **51**, 351–358 (2006).
28. Shepherd, G.M. & Greer, C.A. Olfactory bulb. in *The Synaptic Organization of the Brain,* 4th edn. (ed. Shepherd, G.M.) 159–203 (Oxford University Press, New York, 1998).
29. Aungst, J.L. *et al.* Centre-surround inhibition among olfactory bulb glomeruli. *Nature* **426**, 623–629 (2003).
30. Liu, S., Plachez, C., Shao, Z., Puche, A. & Shipley, M.T. Olfactory bulb short axon cell release of GABA and dopamine produces a temporally biphasic inhibition-excitation response in external tufted cells. *J. Neurosci.* **33**, 2916–2926 (2013).
31. Apicella, A., Yuan, Q., Scanziani, M. & Isaacson, J.S. Pyramidal cells in piriform cortex receive convergent input from distinct olfactory bulb glomeruli. *J. Neurosci.* **30**, 14255–14260 (2010).
32. Davison, I.G. & Ehlers, M.D. Neural circuit mechanisms for pattern detection and feature combination in olfactory cortex. *Neuron* **70**, 82–94 (2011).
33. Mori, K. & Sakano, H. How is the olfactory map formed and interpreted in the mammalian brain? *Annu. Rev. Neurosci.* **34**, 467–499 (2011).
34. Rinberg, D., Koulakov, A. & Gelperin, A. Sparse odor coding in awake behaving mice. *J. Neurosci.* **26**, 8857–8865 (2006).
35. Kato, H.K., Chu, M.W., Isaacson, J.S. & Komiyama, T. Dynamic sensory representations in the olfactory bulb: modulation by wakefulness and experience. *Neuron* **76**, 962–975 (2012).
36. Hopfield, J.J. Odor space and olfactory processing: collective algorithms and neural implementation. *Proc. Natl. Acad. Sci. USA* **96**, 12506–12511 (1999).
37. DasGupta, S. & Waddell, S. Learned odor discrimination in *Drosophila* without combinatorial odor maps in the antennal lobe. *Curr. Biol.* **18**, 1668–1674 (2008).

ONLINE METHODS

Gene targeting. The coding sequence for ChR2(H134R)-YFP (kind gift of G. Nagel, Max Planck Institute for Biophysics) was amplified and cloned into a cassette after an internal ribosome entry site and followed by an autoexcising *neo* selection cassette. The cassette was inserted into an M72 targeting vector[17]. The vector was linearized and electroporated into 129 embryonic stem cells, and correctly targeted clones identified by long-range PCR. Chimeras were generated using targeted clones by aggregation with C57BL/6J morulae. The allele was passed through the male germline, removing the *neo* cassette. M72-ChR2 mice are available from the Jackson Laboratory (#21206, Olfr160<tm1.1(COP4*/EYFP)Tboz>/J).

Mice. Data were collected in 11 male *M72–ChR2-YFP* homozygous mice. Subjects were 6–8 weeks old at the beginning of behavioral training and were maintained on a 12-h light/dark cycle (lights on at 8:00 p.m.) in isolated cages in a temperature- and humidity-controlled animal facility. All animal care and experimental procedures were in strict accordance with a protocol approved by the Howard Hughes Medical Institute Institutional Animal Care and Use Committee.

Sniff recording. To monitor the sniff signal, a 7-mm-long stainless steel cannula (gauge 23, Small Parts capillary tubing) was implanted in the nasal cavity. The cannula was capped between experimental recordings. During experiments, the cannula was connected via polyethylene tubing (801000, A-M systems) to a pressure sensor (24PCEFJ6G, Honeywell) and homemade preamplifier circuit. The signal from the preamplifier was digitized with a microcontroller (Arduino) and acquired by a custom-written data acquisition program written in Python.

Surgery. Mice were anesthetized using isoflurane gas. The head bar, pressure cannula and optical fiber stub were implanted during a single surgery. The sniffing cannula was inserted into a small hole drilled in the bone overlying the nasal cavity, and affixed with glue and stabilized with dental cement. The lateral M72 glomerulus in the right olfactory bulb was found using a fluorescent dissecting microscope, and the overlying bone was thinned. An optical fiber stub was positioned above the glomerulus and fixed in place with glue and dental cement. In the same manner, a control optical fiber stub was implanted above frontal cortex. After surgery, the mouse was caged individually and given at least 3 d for recovery.

Stimulus delivery. For odor stimulus delivery, we used a nine-odor air dilution olfactometer. Odorants (Sigma-Aldrich) were diluted in mineral oil and stored in liquid phase in dark vials. The airflow through the selected odorant vial was diluted another tenfold by the main airflow stream and homogenized in a long thin capillary before reaching the final valve. Between stimuli, a steady stream of 1,000 ml min^{-1} of clean air flowed to the odor port continuously, and the flow from the olfactometer was directed to an exhaust. During stimulus delivery, a final valve (four-way Teflon valve, NResearch) switched the odor flow to the odor port, and diverted the clean airflow to the exhaust. Temporal odor concentration profile was checked by mini PID (Aurora Scientific). The concentration reached a steady state 25–40 ms after final valve opening.

Light stimuli were provided by a 488-nm fiber-coupled laser (Blue Sky Research). The opposite end of the fiber terminated in a ceramic ferrule (Precision Fiber Products), which could be coupled via a phosphor-bronze sleeve (Optequip) to an identical ceramic ferrule holding the optical fiber stub implanted on the mouse. The light stimulus power at the ferrule ending was measured by a power meter (Thorlabs), and calibrated daily by adjusting the amplitude of the pulse to the laser. To prevent the mouse from using leaked light as a visual cue, two bright blue LEDs (Luxeon V-star; Philips Lumileds Lighting) were positioned on either side of the mouse's head, about 1 cm from each eye.

Water delivery was based on gravitational flow controlled by a pinch valve (98302-12, Cole-Parmer) connected via Tygon tubing to a stainless steel cannula (gauge 21, Small Parts capillary tubing), which served as a lick tube. The lick tube was positioned near the mouse's mouth, and could be moved by a micromanipulator. The water volume was calibrated daily to give approximately 2.5 µl per opening. Licks were detected by photodiode beam break by the mouse's tongue.

OSN electrophysiology. Perforated patch recording were made from the dendritic knobs of fluorescently labeled M72-expressing OSNs. The olfactory epithelium from postnatal day 0–14 mice was removed and kept in oxygenated bath solution (95% O$_2$, 5% CO$_2$), containing 124 mM NaCl, 3 mM KCl, 1.3 mM MgSO$_4$, 2 mM CaCl$_2$, 26 mM NaHCO$_3$, 1.25 mM NaHPO$_4$ and 15 mM glucose (pH 7.4). The epithelium was transferred to a recording chamber at 20–23 °C and imaged using an upright DIC microscope (Zeiss Axioskop 2 Plus) equipped with a CCD camera (SensiCam QE, Cooke) and a 40× water-immersion objective. Perforated-patch clamp was performed by including 260 µM amphotericin B in the recording pipette, which was filled with 70 mM KCl, 53 mM KOH, 30 mM methanesulfonic acid, 5 mM EGTA, 10 mM HEPES and 70 mM sucrose (pH 7.2). The electrodes had tip resistances ranging from 8–10 MΩ and liquid junction potentials were corrected in all experiments. Signals were acquired at 10 kHz and low-pass filtered at 2.9 kHz. Odorants were applied via pressure ejection via a multi-barrel pipette placed 20 µm downstream of the cell. Odorants were dissolved in dimethyl sulfoxide (DMSO) and stored at −20 °C. Odorant concentrations were further diluted in bath solution as necessary.

Behavioral control. All behavioral events (odor and final valve opening, laser delivery, water delivery and photobeam crossing) were monitored and controlled by a real-time, Arduino platform–based, behavioral controller box that allowed experimental control with millisecond precision. The behavioral board read trial parameters and sent trial results and streamed sniffing signal to a PC running the custom-written Python program Voyeur (Physion Consulting). Voyeur is a trial-based, behavioral experiment control and acquisition software that allows behavioral protocols to compute parameters of trials and send them to embedded real-time hardware systems. The Arduino code and Python application source is available as a GitHub repository (search for Voyeur in GitHub).

Behavioral procedure and training. Mice were trained as previously described[19]. After at least 3 d of post-operative recovery and at least 7 d of water restriction (1 ml d^{-1}), we began to train the mice. Training sessions took place during the day (mice's dark cycle). Training started with water-sampling sessions, in which the mouse was placed in the head fixation setup and given water for licking. Next, the mice were trained to report odor detection. A behavioral session was broken into pseudo-randomly ordered trials, each of which consisted of a stimulus period, a response period and an intertrial interval (ITI). During the stimulus period, the final valve switched to direct air from the olfactometer to the mouse. Olfactometer flow passed through a vial containing liquid odorant or through a blank vial. Mice received water for licks during the response period following odor delivery and did not receive water if they licked in response to blank delivery. These incorrect licks were punished by lengthened ITI. Correct trial ITIs were 5–7 s, whereas incorrect trial ITIs lasted 10–16 s. Light sessions began after at least two odor detection sessions for each mouse. For initial light training sessions, the stimulus power at the ferrule coupling was 40 mW, whereas the stimulus duration was 10 ms.

After this initial training, mice were trained in the behavioral procedures listed below. Subsets of mice performed in each task, depending on health and the status of their sniff signal (**Supplementary Table 1**). Because the goal of this study was to test whether mice could perform particular discriminations, the number of mice in the sample sufficed to measure this effect. No statistical methods were used to predetermine group sizes. The sample sizes that we chose are similar to those used in previous publications.

For light detection, mice were trained to report detection of light pulses of varying power and 1-ms duration. In mice that maintained a sniff signal, stimuli were delivered at 25 ms after inhalation onset. In mice for which the sniff cannula was blocked, stimuli were delivered at the onset of the stimulus interval.

For light detection in the presence of odor, odorants were diluted 100-fold in mineral oil and tenfold further by air dilution. In each trial, a 500-ms odor pulse was delivered at the onset of the stimulus interval, followed by a 1-ms light pulse. Daily sessions were sequenced: no odor session, M72 ligand session, no odor session, non-M72 ligand session. Light powers were 1 mW or 20 mW, calibrated to evoke criterion performance from each mouse.

For light power discrimination, mice were trained to lick in response to light pulses at a relatively high power (20 mW) and to not lick in response to a range of lower powers (1, 5, and 10 mW). Stimulus durations were 1 ms.

For sniff phase discrimination, mice were trained to lick for stimuli that occurred early in the sniff cycle (25 ms after inhalation onset), and to withhold licking for stimuli that occurred at a range of longer latencies after inhalation onset (125, 75, 50 and 38 ms). Only mice from which a sniff signal could

be recorded were included in these experiments. For fixed-power sniff phase discrimination sessions, the light power was set at 20 mW. For multi-power sniff phase discrimination sessions, light power was 5, 10 or 20 mW. Stimulus durations were 1 ms.

Data analysis. Results of behavioral experiments were analyzed in custom-written programs in Matlab (Mathworks) and Python. Behavioral performance was quantified as a fraction of correct trials. Behavioral performance was compared to chance performance via a two-tailed binomial test, as is appropriate for dichotomous, independent observations. For detection, intensity discrimination and latency difference experiments, each animal's best session is shown. For light detection in the presence of odor, each animal's performance is the mean of three sessions. For multi-power sniff phase discrimination sessions, the mean of five to seven sessions is shown.

Corrigendum: Multiple perceptible signals from a single olfactory glomerulus

Matthew Smear, Admir Resulaj, Jingji Zhang, Thomas Bozza & Dmitry Rinberg

In the version of this article initially published online, ref. 37 and the sentence "In addition, flies can learn to discriminate odors using only a single class of olfactory sensory neuron[37]" in the second paragraph of the Discussion were not present, and the following sentence, concerning the mammalian olfactory system, referred to "learned behavior" rather than simply "behavior." The error has been corrected for the print, PDF and HTML versions of this article.